JOURNAL

OF THE AMERICAN CHEMICAL SOCIETY

VOLUME 104, NUMBER 2 JANUARY 27, 1982

Pressure Dependence of Hydrogen Bonding in Liquid Methanol[1]

William L. Jorgensen*[2] and Mustafa Ibrahim

Contribution from the Department of Chemistry, Purdue University, West Lafayette, Indiana 47907. *Received June 5, 1981*

Abstract: The effects of pressure on the structure, thermodynamic properties, and hydrogen bonding in liquid methanol have been studied via statistical mechanics simulations at 1, 5000, and 15 000 atm. The intermolecular interactions were described by the previously reported transferable intermolecular potential functions (TIPS) which include Lennard–Jones and Coulomb terms. The thermodynamic results are found to be in good agreement with experiment; particularly, the density is within 4–6% of experimental data across the entire pressure range. Although the range corresponds to a compression of 30%, the hydrogen bonding is essentially unaffected. This is in accord with the pressure dependence of IR and Raman spectra of liquid alcohols. The decrease in volume occurs primarily between the hydrogen-bonded chains with the chains themselves remaining unaltered. The observation is reflected in the interesting behavior of the radial distribution functions (rdfs). The first peaks in the rdfs that characterize the hydrogen bonding (g_{OO}, g_{OH}, and g_{HH}) are suppressed by increasing pressure, while the peaks in the rdfs involving the methyl groups are enhanced. Stereo plots and numerous distributions for the energetics and hydrogen bonding provide a thorough description of the liquid's structure at the molecular level.

Under standard conditions, application of 15 000 atm of pressure to an organic liquid yields a compression of ca. 30%. It is fundamentally interesting to consider the concomitant thermodynamic and structural effects on the liquid. Experimentally, the structural changes have been studied by various spectroscopic methods including Raman and IR using ruby or diamond anvil cells.[3-7] The appropriate theoretical approaches for obtaining detailed structural information at the molecular level are to perform molecular dynamics or Monte Carlo statistical mechanics simulations for the liquid in the isothermal, isobaric (NPT) ensemble. However, such calculations are still relatively uncommon, and, in fact, the only simulations that have been reported for a molecular liquid above 1 atm are our recent Monte Carlo studies for *n*-butane.[8] The results of this work were very encouraging. Specifically, the computed thermodynamic properties were in excellent agreement with experiment; in particular, the error in the computed density was less than 3% from 1 to 15 000 atm. Furthermore, increased pressure was found to provide a small shift in the conformational equilibrium toward higher gauche population which is in accord with Raman data on lower *n*-alkane liquids.[4,8]

A key problem in liquid simulations is the need for potential functions to accurately describe the interactions between monomers in the fluids. Consequently, we have developed a set of simple, transferable intermolecular potential functions (TIPS)[9] that were shown to yield good thermodynamic, structural, and conformational results for liquid alcohols,[10,11] ethers,[12] *n*-butane,[8,13] and 1,2-dichloroethane[13] in Monte Carlo simulations. Except for *n*-butane[8] and dimethyl ether,[12] the computations have been performed in the NVT ensemble. Although the computed densities for these two liquids are in good agreement with experiment, it is important to establish whether the TIPS also yield reasonable densities for the other types of liquids. An obvious extension of such simulations is to study dilute solutions, solvation and solvent effects in organic chemistry. Clearly, the results of the dilute solution simulations would not be very meaningful if the solvent desired a density significant different than observed experimentally.

(1) Quantum and statistical mechanical studies of liquids 20.
(2) Camille and Henry Dreyfus Foundation Teacher-Scholar, 1978–1983; Alfred P. Sloan Foundation Fellow, 1979–1981.
(3) For a review, see: Weigang, O. E.; Robertson, W. W. In "High Pressure Physics and Chemistry"; Bradley, R. S., Ed.; Academic Press: New York, 1963; Vol. 1, p 177.
(4) Schoen, P. E.; Priest, R. G.; Sheridan, J. P.; Schnur, J. M. *J. Chem. Phys.* **1979**, *71*, 317. Wunder, S. L.; Cavatorta, F.; Priest, R. G.; Schoen, P. E.; Sheridan, J. P.; Schnur, J. M. *Polym. Prep., Am. Chem. Soc., Div. Polym. Chem.* **1979**, *20*, 770. Wunder, S. L.; Schoen, P. E.; Schnur, J. M.; to be published.
(5) (a) Fishman, E.; Drickamer, H. G. *J. Chem. Phys.* **1956**, *24*, 548. (b) Benson, A. M.; Drickamer, H. G. *Ibid.* **1957**, *27*, 1164. (c) Wiederkehr, R. R.; Drickamer, H. G. *Ibid.* **1958**, *28*, 311.
(6) Collins, J. R. *Phys. Rev.* **1930**, *36*, 305.
(7) (a) Jakobsen, R. J.; Mikawa, Y.; Brasch, J. W. *Appl. Spectrosc.* **1970**, *24*, 333. (b) Mammone, J. F.; Sharma, S. K.; Nicol, M. *J. Phys. Chem.* **1980**, *84*, 3130.
(8) Jorgensen, W. L. *J. Am. Chem. Soc.* **1981**, *103*, 4721.
(9) Jorgensen, W. L. *J. Am. Chem. Soc.* **1981**, *103*, 335.
(10) Jorgensen, W. L. *J. Am. Chem. Soc.* **1981**, *103*, 341.
(11) Jorgensen, W. L. *J. Am. Chem. Soc.* **1981**, *103*, 345.
(12) Jorgensen, W. L.; Ibrahim, M. *J. Am. Chem. Soc.* **1981**, *103*, 3976.
(13) Jorgensen, W. L. *J. Am. Chem. Soc.* **1981**, *103*, 677. Jorgensen, W. L.; Binning, R. C.; Bigot, B. *J. Am. Chem. Soc.* **1981**, *103*, 4393.
(14) (a) Bridgman, P. W. *Proc. Amer. Acad. Arts Sci.* **1942**, *74*, 399. (b) *Ibid.* **1913**, *49*, 3. (c) Piermarine, G. J.; Block, S.; Barnett, J. D. *J. Chem. Phys.* **1973**, *44*, 5377.

0002-7863/82/1504-0373$01.25/0

Thus, the simulations of liquid methanol described here at 25 °C and 1, 5000, and 15 000 atm were undertaken for several reasons: to study in detail the effects of pressure on the thermodynamics and structure of a prototype hydrogen-bonded liquid, to further test the viability of performing liquid simulations at high pressure, and to further evaluate the utility of the TIPS. The results are again gratifying as the computed density is within 4–6% of experiment across the pressure range. The structural results are also in accord with IR, Raman, and X-ray data as discussed below. An extensive analysis of the hydrogen bonding reveals a remarkable insensitivity to pressure; the compression occurs predominantly between the hydrogen-bonded chains. To begin, the computational details will be presented followed by the results and discussions for the properties and distribution functions.

Monte Carlo Simulations

The statistical mechanics calculations were carried out at 25 °C in the NPT ensemble. The computational formalism and procedure were identical with those previously described for *n*-butane[8] and will not be repeated here.

The TIPS previously reported for alcohols were used in this work.[9] Each methanol monomer is represented by three interaction sites centered on the carbon, oxygen, and hydroxyl hydrogen with the methyl hydrogens implicit. The sites interact intermolecularly via Lennard–Jones and Coulomb terms (eq 1). A^2 for methyl

$$\epsilon_{mn} = \sum_{i}^{\text{on } m} \sum_{j}^{\text{on } n} \frac{q_i q_j e^2}{r_{ij}} + \frac{A_i A_j}{r_{ij}^{12}} - \frac{C_i C_j}{r_{ij}^{6}} \qquad (1)$$

and oxygen is 7.95×10^6 and 5.15×10^5 kcal Å^{12}/mol and the corresponding C^2 parameters are 2400 and 600 kcal Å^6/mol, while A and C for hydrogen are zero.[9] The charges are 0 (−0.685 e), CH_3 (+0.285 e), and H_O (+0.40 e). This yields a dipole moment of 2.21 D using the standard geometries which are employed throughout (r(OH) = 0.945 Å, r(CO) = 1.430 Å, ∠COH = 108.5°). The TIPS results for dimers were described in detail previously.[9] For methanol, the lowest energy dimer has the linear hydrogen-bonded form characterized by r(OO) = 2.79 Å, θ = 27°, and a dimerization energy of 5.68 kcal/mol.[9]

The Monte Carlo calculations were executed by using cubic samples of 128 monomers, periodic boundary conditions, Metropolis sampling, and applied pressures of 1, 5000 and 15 000 atm. Spherical cutoffs at 10.0, 9.5, and 9.0 Å were used in evaluating the dimerization energies for the three runs, respectively. The shortening was necessitated by progressive reduction in the average length of an edge of the periodic cube. In each case interactions with a monomer's ca. 60 nearest neighbors were included. Cutoff corrections for the Lennard–Jones portion of the energy were made as usual[9] and amounted to −0.16, −0.23, and −0.31 kcal/mol for the runs at 1, 5K, and 15K atm. New configurations were created by randomly selecting a monomer, translating it randomly in all three Cartesian directions, and randomly rotating it about a randomly selected axis. The volume of the system was changed randomly on every 400th move, and all intermolecular distances were scaled accordingly. The ranges for the motions were selected to yield acceptance rates of 40–50% for new configurations. For the simulations at 1, 5K, and 15K atm the ranges for the translations were ±0.17, ±0.15, and ±0.13 Å, the ranges for the rotation ±17, ±15, and ±13°, and the ranges for the volume moves ±250, ±175, and ±110 Å^3, respectively. The ranges had to be reduced due to the higher density at higher pressure in order to keep the acceptance rates similar.

The simulation at 1 atm was initiated from the last configuration in the previous NVT run for liquid methanol.[10] Since the error in the density was small, convergence of the energy and volume were rapid and occurred within 200K configurations. Final averaging took place over an additional 500K configurations in this case. The higher pressures were achieved gradually in increments of ca. 1K atm per 10K configurations. For the run at 5K atm, a total off 1300K configurations were generated. Equilibration was complete in about 500K configurations, though the averaging was only over the final 650K. At 15K atm, 1250K configurations were utilized, 550K for equilibration and 700K for averaging.

Table I. Thermodynamic Results for Liquid Methanol at 25 °C

property	pressure, atm: 1	5000	15000
V, Å^3	71.6 ± 0.5	57.9 ± 0.2	50.5 ± 0.1
V(exptl), Å^3	67.6[a,b]	55.0[a]	48.7[a]
$-E^{inter}$, kcal/mol	7.05 ± 0.04	7.59 ± 0.04	7.40 ± 0.03
ΔH_{vap}, kcal/mol	7.51 ± 0.04		
ΔH_{vap}(exptl)	8.94 ± 0.03[b]		
κ, atm^{-1} × 10^{-6}	105 ± 27	25 ± 6	9 ± 1
κ(exptl)	118[a]	16[a]	6[a]
C_P, cal/(mol deg)	23 ± 3	23 ± 3	20 ± 2
C_P(exptl)	19.4[b]	19[a,b]	
α, deg^{-1} × 10^{-5}	102 ± 35	52 ± 21	27 ± 8
α(exptl)	118[a]	48[a]	32[a]

[a] Reference 14. See also the text. [b] Reference 15.

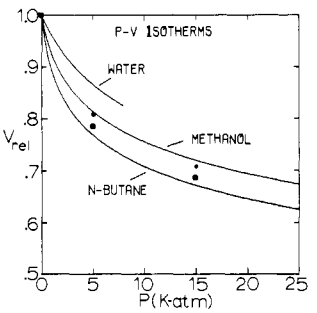

Figure 1. The relative volumes of liquid water (25 °C), methanol (25 °C), and *n*-butane (0 °C) as a function of pressure. The curves are experimental data and the dots and squares are results of Monte Carlo calculations for methanol and *n*-butane,[8] respectively.

Every 2500th configuration was stored during the averaging for subsequent analyses of the hydrogen bonding as discussed below.

The calculations were executed in part on a CDC/6600 at the Purdue University Computing Center and primarily on a Harris Corp. H-80 computer in our laboratory. Roughly 300K configurations could be run per day on the H-80 which has a floating point hardware unit.

Results and Discussion

(a) Thermodynamics. The thermodynamic results from the Monte Carlo calculations are compared with experimental values in Table I. The error bars reported for the computed properties are ±2σ and were obtained from separate averages over each ca. 40K configurations.

The experimental density at 25 °C and 1 atm, 0.7866 g cm^{-3},[15] implies a molecular volume of 67.6 Å^3 which is 5.9% lower than the computed value of 71.6 Å^3. The results at the higher pressures are also in good agreement with experiment; the errors are 5.3% at 5K atm and 3.7% at 15K atm. The data are illustrated in Figure 1 which shows the relative volumes of water and methanol at 25 °C and of *n*-butane at 0 °C as a function of pressure. The curves for water[16] and methanol[14] are experimental data, while the curve for *n*-butane is estimated from experimental data on many higher *n*-alkanes.[8] The curve for liquid water terminates near 8K atm since that is the freezing point. Methanol freezes near 35K atm at 25 °C, though the superpressed liquid has been studied up to 92K atm.[7,14] The dots and squares in Figure 1 show the computed results for methanol and *n*-butane[8] normalized to a relative volume of 1 at 1 atm. Though the data are limited, the computed isotherms appear to nicely mirror the experimental curves. Not surprisingly from a structural standpoint, the compressibility of methanol is intermediate between that of water and that of a hydrocarbon. Liquid methanol is reduced in volume by 19% in going to 5K atm and by another 9% at 15K atm. The isotherm becomes relatively flat beyond this point, and the volume

(15) Wilhoit, R. C.; Zwolinski, B. J. *J. Phys. Chem. Ref. Data, Suppl.* **1973**, *1*, 2.
(16) Grindley, T.; Lind, J. E. *J. Chem. Phys.* **1971**, *54*, 3983.

is only reduced an additional 10% in continuing to 50K atm.[14a]

The experimental values for the isothermal compressibility, κ, and coefficient of thermal expansion, α, were obtained from Bridgman's data.[14] For κ, this entailed fitting his PV data at 25 °C to the Tait equation (2) which then gives $\kappa = C/[2.303(B + P)]$. The least-squares program yielded an excellent fit for the 15 data points between 0 and 50K atm with $C = 0.2143$, $B = 780.8$ atm, and a σ of 0.003 $\Delta V/V_0$. For α, Bridgman's data at constant pressure were fit to eq 3 from which $\alpha = (\partial V/\partial T)_P/V$. The α

$$\Delta V/V_0 = C \log [(B + P)/(B + P_0)] \quad (2)$$

$$V = V_0[1 + at + bt^2 + ct^3] \quad (3)$$

at 1 atm obtained in this fashion (118×10^{-5}/deg) is in good agreement with a recent, independent experimental estimate, 119.5×10^{-5}/deg.[17] Overall, the computed values of α and κ at all three pressures are in excellent agreement with the experimental data in Table I in view of the error bars.

The remaining fluctuation property is the heat capacity, C_P, which is computed as the sum of an unimolecular term approximated by the heat capacity of the ideal gas (10.5 cal/(mol deg))[15] and of an intermolecular term obtained from the fluctuation of the enthalpy during the liquid simulation. Again the results are in close agreement with experiment. The relative insensitivity of C_P to pressure is a general phenomenon for organic liquids[14b] and contrasts the behavior of α and κ.

As shown in Table I, the intermolecular energy decreases significantly in going from 1 to 5K atm and then rises somewhat in continuing to 15K atm. The same pattern was found for *n*-butane[8] and is also typical of a wide variety of organic liquids as Bridgman discovered in 1913.[14b] In fact, he found that the energy of an organic liquid is often minimized near a relative volume of 0.8 which corresponds to pressures near 5K atm at normal temperatures. At this point, the intermolecular attractions are optimized. However, further compression leads to an increase in repulsive van der Waal's interactions (vide infra).

The heat of vaporization was computed as usual: $\Delta H_V = -E^{inter}(l) + P(V°(g) - V(l)) - (H°(g) - H(g))$. The last term is the enthalpy departure function for the real gas and amounts to 0.13 kcal/mol.[15] The most serious assumption here is that the vibrational energy for a monomer in the liquid and the ideal gas are the same. This is certainly not true for a hydrogen-bonded liquid: substantial shifts ($\sim$300 cm^{-1}) to lower frequencies are observed for the O–H stretch in alcohols in going from the gas to the liquid.[18] Although the zero-point energy for the gas should be higher than for the liquid, an unambiguous estimate of the difference is difficult to make. A correction on the order of 1 kcal/mol for methanol would not seem unreasonable. In view of this, the fact that the computed ΔH_V underestimates the experimental value by 1.4 kcal/mol (16%) is not surprising. The other likely contributor to the discrepancy is the neglect of three-body effects inherent in the two-body TIPS. The three-body effects arise from enhanced polarization of the monomers upon hydrogen-bond formation and are constructive.[9-11] Both this effect and the vibrational energy change should be relatively insignificant for the non-hydrogen-bonded liquids which is consistent with the excellent heats of vaporization computed in these cases with the TIPS.[8,12,13]

Overall, the thermodynamic results reflect a reasonable model for liquid methanol. The trends in all computed properties as a function of pressure are in accord with experimental observations. The absolute errors for the computed properties are also small except apparently for the heat of vaporization where the 16% error may be partly alleviated by an appropriate vibrational energy correction. Alternatively, the volume and energy could both be lowered by deepening the hydrogen bonding well in the TIPS, a procedure which would help compensate for the neglected three-body effects. Unfortunately, this tends to overly structure the first shell of neighbors as reflected in the radial distribution functions.[10] Thus, it appears that the TIPS provide a reasonable compromise in a two-body format.

(17) Hales, J. L.; Ellender, J. H. *J. Chem. Thermodyn.* **1976**, *8*, 1177.

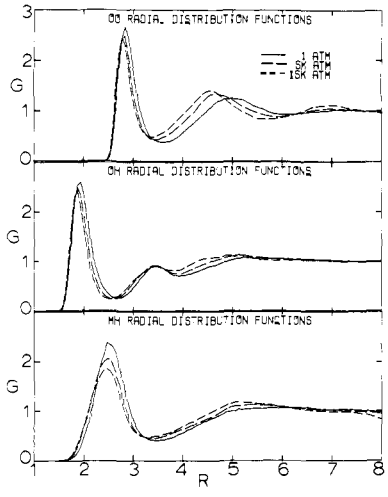

Figure 2. The OO, OH, and HH radial distribution functions computed for liquid methanol at 25 °C. Distances are in Å throughout.

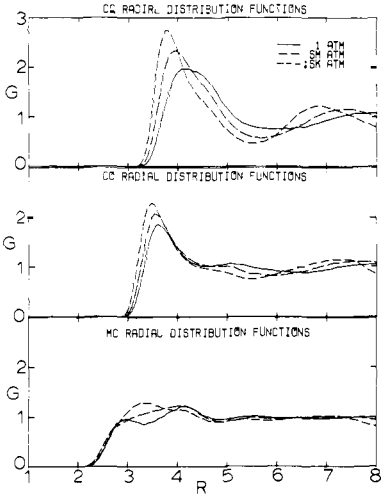

Figure 3. The CC, CO, and CH_O radial distribution functions computed for liquid methanol.

(b) Structure. Since the error in the density is small, the results from the previous NVT simulation which enforced the experimental density are essentially identical with the results found here at 1 atm.[10] Thus, the focus here will be on the changes in structure with pressure. It was previously shown that the NVT results for the radial distribution functions (rdfs) are in accord with the available X-ray data on the peak positions and areas.[10] The peak heights also seem reasonable on the basis of more refined diffraction data for liquids such as water[9] and ammonia.[19]

The OO, OH, and HH rdfs obtained at the three pressures are displayed in Figure 2. As discussed previously, the liquid's structures is dominated by hydrogen-bonded chains whose windings appear uncorrelated.[10,20] The first peaks in these distributions reflect the nearest, hydrogen-bonded neighbors for a monomer as does the second peak for the OH rdf. The more distant peaks correspond to both inter- and intrachain remote neighbors. Interestingly, the peaks for the hydrogen-bonded neighbors are lowered and shifted to slightly shorter intermolecular separation as the pressure increases. This contrasts the results for liquid *n*-butane in which the first peaks in the rdfs all increased in height.[8] However, the integrals of the first peaks for methanol vary little, e.g., for g_{OO} the first peak contains 1.96, 2.04, and 2.17

(18) (a) Luck, W. A. P. In "The Hydrogen Bond"; Schuster, P., Zundel, G., Sandorfy, C., Eds.; North-Holland Publishing Co.: Amsterdam, 1976; Vol. 3, Chapter 28. (b) Hallam, H. E. *Ibid.* Chapter 22.
(19) Jorgensen, W. L.; Ibrahim, M. *J. Am. Chem. Soc.* **1980**, *102*, 3309.
(20) Jorgensen, W. L. *J. Am. Chem. Soc.* **1980**, *102*, 543.

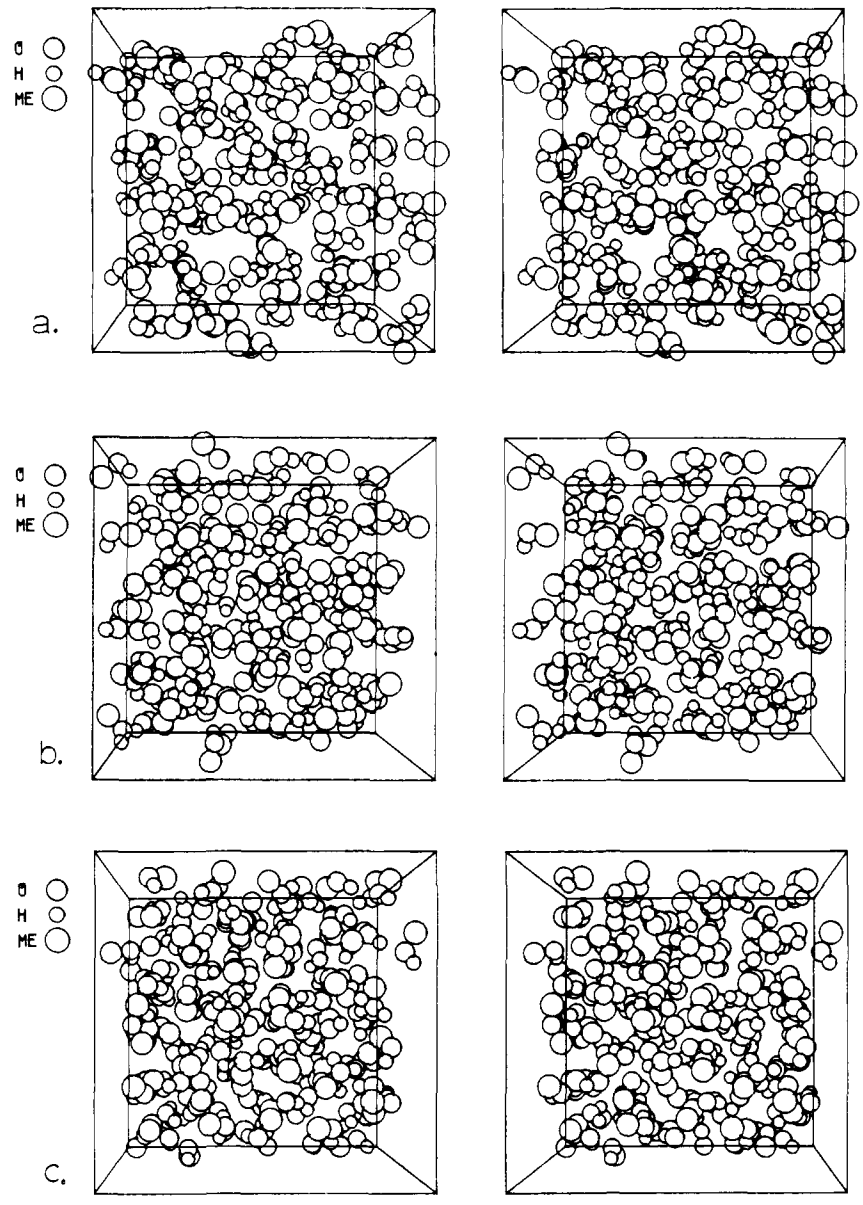

Figure 4. Stereo plots of configurations from the Monte Carlo simulations of liquid methanol at (a) 1 atm, (b) 5000 atm, and (c) 15,000 atm. For comparison, the cube corresponds to the boundary of the periodic cube for the configuration at 1 atm.

neighbors at 1, 5K, and 15K atm. The peak lowering states that relative to the bulk density the hydrogen bonding shows less structure as the pressure rises. In fact, as proven below, the hydrogen bonding and chain structure are essentially unaffected over the pressure range. So, since the bulk density is increasing, the hydrogen bonding shows less structure relative to the bulk and the first peaks are somewhat suppressed. Consistently, the outer peaks are sharpened since they involve interchain contributions. The compression occurs primarily between, not along, the chains so more efficient packing increases the interchain structure similar to the findings for liquid *n*-butane.[8]

The analysis is supported by the results for the CC, CO, and CH rdfs shown in Figure 3. Except for the first peak in the CH function which is due to a hydrogen bond donating neighbor, the peaks for these rdfs all involve inter and intra-chain contacts. Therefore, the tighter interchain packing causes the peaks to sharpen and shift to shorter separation with increasing pressure. In summary, higher pressure increases the interchain structure but has little effect on the intrachain structure and hydrogen bonding.

This notion is further illustrated by the stereo plots in Figure 4. One view of the periodic cube for the last configuration of each run is shown. For comparison, the cubes in the drawings show the actual boundary of the periodic cube for the configuration at 1 atm. Consequently, the monomers fill less of the cube as the pressure increases which reflects the compression. Clearly, hydrogen-bonded chains are ubiquitous in the drawings. Moreover, the free space between the chains at 1 atm is significantly reduced at the higher pressures, while the local hydrogen bonding remains intact and relatively unperturbed.

In closing this section, it should again be pointed out that the chain structure in the liquid is more complicated than in the solid where each monomer has exactly two hydrogen-bonded neighbors.[10,20,21] The distributions of neighbors within the range of the first peak of the 00 rdfs for the liquid were obtained from the saved configurations and are shown in Figure 5. Although the average coordination number is 2, only about 60% of the monomers have exactly two neighbors with the rest roughly split between having one and three neighbors. The effect of pressure on the distribution is modest, though a gradual shift toward higher coordination numbers is apparent.

(c) Energy Distributions. The distributions for the total intermolecular bonding energies for monomers in liquid methanol are illustrated in Figure 6. The unimodal distributions have similar shape, though some broadening is apparent with increasing pressure. For *n*-butane, the broadening was pronounced;[8] however,

(21) Tauer, K. J.; Lipscomb, W. N. *Acta Crystallogr.* **1952**, *5*, 606.

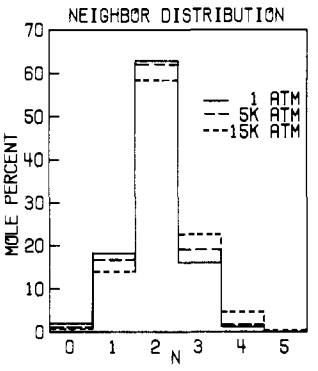

Figure 5. Distribution of neighbors within the first peaks of the OO radial distribution functions for liquid methanol.

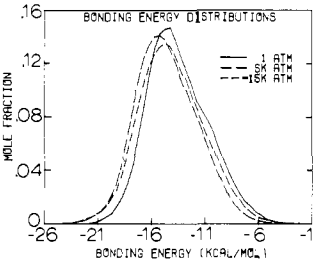

Figure 6. Total bonding energy distributions for monomers in liquid methanol. Units for the ordinate are mole fraction per kcal/mol.

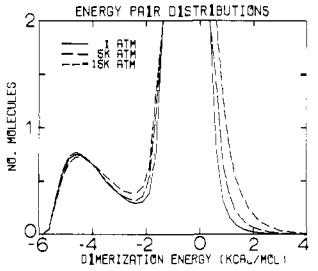

Figure 7. Distributions of dimerization energies for a monomer in liquid methanol. Units for the ordinate are number of molecules per kcal/mol.

the energetics for methanol are strongly influenced by the hydrogen bonding which is little affected by the pressure change. The distributions in Figure 6 are consistent with the intermolecular energies in Table I that were discussed above. Specifically, the intermolecular bonding in the liquid is most attractive at 5K atm.

The distributions of dimerization energies that a monomer experiences on the average are shown in Figure 7. The spikes near 0 kcal/mol are due to the weak interactions with the many distant molecules in the bulk. The most interesting feature is the peak at low energy which is due to the monomer's hydrogen-bonded neighbors.[9-11] This peak and, therefore, the hydrogen bonding are altered little by increasing pressure. The minimum occurs at −2.375 kcal/mol for 1 and 5K atm and at −2.50 kcal/mol for 15K atm. As before, the position of the minimum may be used as a convenient energetic limit for hydrogen bonding. Integration to this point then yields the average numbers of hydrogen bonds per monomer as 1.71, 1.75, and 1.69 for 1, 5K, and 15K atm, respectively. These values are clearly very sensitive to the integration limit; extending it to about −1.85 kcal/mol would yield averages of two hydrogen bonds per monomer. A related, even more sensitive concept is the average chain length for the hydrogen bonded multimers. For chains with perfect two coordination, the average length $l = 2/(2 - n)$ where n is the average number of hydrogen bonds. This function varies rapidly in the vicinity of $n = 2$, so for $n = 1.75$, $l = 8$ and for $n = 2$, $l = \infty$. In view of this sensitivity and the complications due to chain branching, fruitful discussions of chain length in the liquid phase are generally elusive though it has been a common topic in the spectroscopic literature.[7a,18]

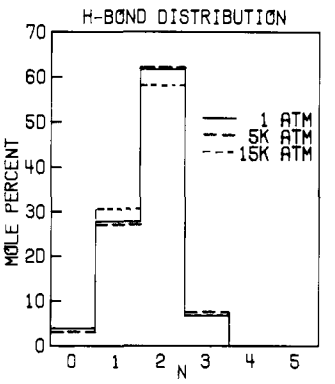

Figure 8. Distributions of hydrogen bonds for monomers in liquid methanol.

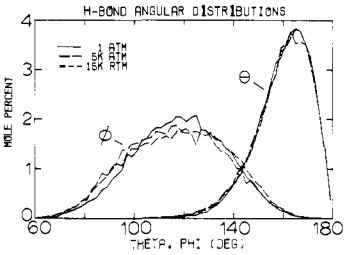

Figure 9. Distributions for the hydrogen bonding angles θ (O—H···O) and ϕ (H···O—H) in liquid methanol. The units for the ordinate are mole percent per degree.

Table II. Results of Hydrogen Bond Analysis for Liquid Methanol at 25 °C[a]

property	pressure, atm			
	1	5000	15 000	
⟨no. of H bonds⟩	1.71	1.75	1.69	1.74
ϵ_{HB}^{max}	−2.375	−2.375	−2.500	−2.375
$\langle\epsilon_{HB}\rangle$	−4.12	−4.11	−4.07	−4.03
$\langle\epsilon_{Coulomb}\rangle$	−4.56	−4.73	−4.90	−4.85
$\langle\epsilon_{L-J}\rangle$	0.44	0.62	0.83	0.82
% monomers in N H bonds				
$N = 0$	3.9	3.0	3.9	3.2
$N = 1$	27.7	27.0	30.7	28.5
$N = 2$	61.7	62.3	58.4	60.0
$N = 3$	6.8	7.6	6.8	7.9
$N = 4$	0.0	0.1	0.3	0.4

[a] ϵ's in kcal/mol. ϵ_{HB}^{max} is the maximum hydrogen bond energy. $\epsilon_{Coulomb}$ and ϵ_{L-J} are the contributions of the Coulomb and Lennard-Jones interactions to the hydrogen bond energy, ϵ_{HB}.

(d) Hydrogen Bonding Analyses. As in the past, the hydrogen bonding in the saved configurations was analyzed using the energetic definitions of a hydrogen bond set by the locations of the minima in the energy pair distributions.[9-11,19,20] The distributions of hydrogen bond numbers are shown in Figure 8 and recorded in Table II. The table contains results at 15K atm using both a cutoff at −2.500 and −2.375 kcal/mol. The former figure corresponds to the minimum and the latter is the same as for the runs at 1 and 5K atm. There is little difference between the two sets of results for 15K atm in Table II. With these energetic definitions, roughly 60% of the monomers are found to participate in two hydrogen bonds, 30% in one hydrogen bond, and 8% in three hydrogen bonds. These environments correspond to monomers interior to the chains, chain ends, and branch points (Y junctions) in the chains, respectively.[10,20] In view of the statistical uncertainties and the choice of cutoff, increasing pressure to 15K atm has no effect on the hydrogen bond distributions and, therefore, the chain structure. This is confirmed by the constancy of the computed hydrogen bond angle distributions shown in Figure 9 where θ is the O—H···O angle and ϕ is the H···O—H angle.

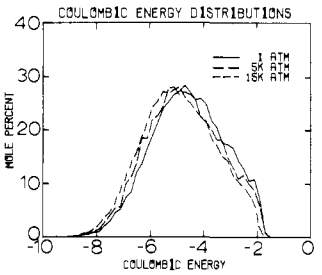

Figure 10. Distributions for the Coulombic energy contributions to the hydrogen bonds. Units for the ordinate are mole percent per kcal/mol.

These observations are also consistent with the pressure dependence of IR and Raman spectra for a variety of pure liquid alcohols including methanol.[6,7] Though modest IR frequency shifts are observed in the liquids, they are comparable to those for the solids which led to the conclusion that in the liquids "pressure variations do not affect the polymer equilibrium".[7a] Furthermore, the C—O stretching vibration for liquid methanol is essentially unchanged in Raman spectra up to 20 kbar.[7b] Thus, little change in the backbone of the hydrogen-bonded chains is indicated.[7b] It should be noted that the behavior of alcohols in dilute solution with nonpolar solvents is different. In this case, increased polymerization is observed at higher pressure as could be anticipated from the decrease in volume accompanying hydrogen bond formation.[5] Also, in contrast to methanol, substantial hydrogen bond distortion is anticipated upon compression of liquid water.[22] The only other mode available is distortion of the monomers which is a much higher energy process.

Some new analyses of the energetics for the hydrogen bonding were also carried out. In view of the form of the TIPS (eq 1), the hydrogen bonding can be broken into separate Lennard–Jones and Coulomb terms. As summarized in Table II, at 1 atm the average hydrogen bond energy is −4.12 kcal/mol which consists of an attractive Coulombic contrbituion of −4.56 kcal/mol and a repulsive contribution of +0.44 kcal/mol from the Lennard–Jones terms. The average hydrogen bond energy remains nearly constant with increasing pressure which results from a cancellation of the Coulomb contribution becoming a little more attractive and the Lennard–Jones term more repulsive. This is consistent with the slight shortening in the hydrogen bond lengths with increasing pressure that is reflected in the shifting of the maxima for the first peaks in the OO and OH rdfs (Figure 2). The red-shift with increasing pressure for the O—H vibrations in liquid and solid alcohols has been interpreted sometimes as reflecting a strengthening of the hydrogen bonds.[7b,23] The present results question this association. The red-shifts may be due to shortening of the hydrogen bonds, but the shortening does not assure the bonds' strengthening. It may also be noted that our results do not support the suggestion that the observed decrease in the Kirkwood g factor for liquid methanol up to 3 kbar is due to

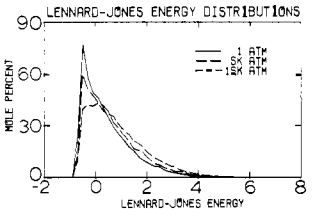

Figure 11. Distributions for the Lennard–Jones energy contributions to the hydrogen bonds. Units are the same as in Figure 10.

"destruction of relatively voluminous hydrogen bonded associates by high pressures".[24]

The separate distributions for the Coulomb and Lennard–Jones contributions to the hydrogen bond energies are shown in Figures 10 and 11. The Coulombic energies like the total bonding energies (Figure 6) more or less symmetrically cover an energy range, while the Lennard–Jones distribution is skewed toward lower energy. The difference in shapes is likely due to the shorter range nature of the Lennard–Jones potentials than the Coulomb interactions. It also implies that although the hydrogen bonding is dominated by the Coulombic interactions, there is a tendency to keep the Lennard–Jones interactions as favorable as possible.

Two final notes on the energetics can be made. First, from Table II it is clear that hydrogen bonding contributes an average of about 8 kcal/mol to the total bonding of about 14–15 kcal/mol (Figure 6) for a monomer is liquid methanol. Thus, the interactions with the many more remote neighbors make a contribution to the bonding almost as significant as the hydrogen bonding. Secondly, it is important to emphasize that the energies and geometries for the hydrogen bonds are smoothly distributed over substantial ranges as illustrated in Figures 7 and 9.

Conclusion

The present results further demonstrate that meaningful theoretical studies of complex organic liquids can be performed under high-pressure conditions and that thorough structural descriptions of the liquids can be obtained at the molecular level. The quality of thermodynamic and structural results for liquid methanol reported here also provide additional support for the utility of the simple TIPS for describing intermolecular interactions.[25] An interesting specific finding for liquid methanol is that the hydrogen bonding and chain structure are essentially unaffected by pressures up to 15 000 atm; the compression occurs predominantly between the hydrogen-bonded chains.

Acknowledgment. Gratitude is expressed to the National Science Foundation (Grant CHE-8020466) for support of this work and to Yarmouk University, Irbid, Jordan, for a fellowship granted to M.I. We are also grateful to Dr. Phillip Cheeseman for use of his stereo plotting program.

Registry No. Methanol, 67-56-1.

(22) (a) Kamb, B. In "Water and Aqueous Solutions"; Horne, R. A., Ed.; Wiley: New York, 1972; p 9. (b) Kanno, H.; Speedy, R. J.; Angell, C. A. *Science (Washington, D.C.)* 1975, *189*, 880. Angell, C. A.; Kanno, H. *Ibid.* 1976, *193*, 1121.

(23) Jakobsen, R. J.; Brasch, J. W.; Mikawa, Y. *J. Mol. Struct.* **1967**, *1*, 309.

(24) Franck, E. U.; Deul, R. *Discuss. Faraday Soc.* **1978**, *66*, 191.

(25) The MHL potential function reported for the methanol dimer[10] was also used in an NPT simulation of the liquid at 1 atm. This function is more complicated than the TIPS and significantly slower to use since it includes the methyl hydrogens explicitly. The thermodynamic results with the MHL function are slightly better than with the TIPS; e.g., the error for the computed density is 4% vs. 6%.